

## Facile Synthesis of Gold Nanoparticles with Narrow Size Distribution by Using AuCl or AuBr as the Precursor

Xianmao Lu,<sup>[a]</sup> Hsing-Yu Tuan,<sup>[b]</sup> Brian A. Korgel,<sup>[c]</sup> and Younan Xia\*<sup>[a]</sup>

**Abstract:** Gold(I) halides, including AuCl and AuBr, were employed for the first time as precursors in the synthesis of Au nanoparticles. The synthesis was accomplished by dissolving Au<sup>I</sup> halides in chloroform in the presence of alkylamines, followed by decomposition at 60 °C. The relative low stability of the Au<sup>I</sup> halides and their derivatives eliminated the need for a reducing agent, which is usually required for Au<sup>III</sup>-based precursors to generate Au nanoparticles. Controlled growth of Au nanoparticles with a narrow size distribution was achieved when AuCl and

oleylamine were used for the synthesis. FTIR and mass spectra revealed that a complex, [AuCl(oleylamine)], was formed through coordination between oleylamine and AuCl. Thermolysis of the complex in chloroform led to the formation of dioleylamine and Au nanoparticles. When oleylamine was replaced with octadecylamine, much larger nanoparticles were obtained due to the lower stability of [AuCl(octade-

cylamine)] complex relative to [AuCl(oleylamine)]. Au nanoparticles can also be prepared from AuBr through thermolysis of the [AuBr(oleylamine)] complex. Due to the oxidative etching effect caused by Br<sup>-</sup>, the nanoparticles obtained from AuBr exhibited an aspect ratio of 1.28, in contrast to 1.0 for the particles made from AuCl. Compared to the existing methods for preparing Au nanoparticles through the reduction of Au<sup>III</sup> compounds, this new approach based on Au<sup>I</sup> halides offers great flexibility in terms of size control.

**Keywords:** alkylamines • complexes • gold • nanoparticles

### Introduction

Among all nanostructured materials, Au nanoparticles with sizes ranging from 1.5 to ≈100 nm are probably the most extensively studied systems as a result of their intriguing properties and fascinating applications.<sup>[1]</sup> The excellent chemical stability, biocompatibility, surface plasmon resonance effect, and unique catalytic activity associated with Au nanoparticles have enabled a broad range of applications in areas that include biomedical research,<sup>[2]</sup> electronics,<sup>[3]</sup> information

storage,<sup>[4]</sup> and photovoltaic devices.<sup>[5]</sup> Notable examples include cancer diagnosis,<sup>[6]</sup> molecular ruler,<sup>[7]</sup> DNA sequence detection,<sup>[8]</sup> low-temperature catalysis for the conversion of CO to CO<sub>2</sub>,<sup>[9]</sup> as well as thermal<sup>[10]</sup> and colorimetric<sup>[11]</sup> sensing. Not surprisingly, these and other applications have fueled research related to the preparation of Au nanoparticles with controllable sizes, diverse morphologies, and assorted functionalities.<sup>[12]</sup>

The first synthesis of Au colloids was reported ≈150 years ago by Michael Faraday who used phosphorous to reduce AuCl<sub>4</sub><sup>-</sup> ions.<sup>[13]</sup> Since then, many methods based on the reduction of Au<sup>III</sup> salts have been developed by various researchers. For instance, Turkevich employed a mild reducing agent, sodium citrate, to form Au colloids in aqueous solution from AuCl<sub>4</sub><sup>-</sup>.<sup>[14]</sup> In 1994, another milestone was achieved in the synthesis of Au nanoparticles by the Brust group.<sup>[15]</sup> In their work, Au nanoparticles with relatively narrow polydispersities and controllable sizes were obtained by reducing AuCl<sub>4</sub><sup>-</sup> with NaBH<sub>4</sub> in the presence of a capping ligand, dodecanethiol, and a phase transfer agent, tetraoctylammonium bromide. As elemental Au can be easily generated by reducing the salts of Au ions, many different reducing agents, including hydrazine,<sup>[16]</sup> amines,<sup>[17]</sup> alcohols,<sup>[18]</sup> polymers,<sup>[19]</sup> and even fungus,<sup>[20]</sup> in addition to the

[a] Dr. X. Lu, Prof. Y. Xia  
Department of Biomedical Engineering  
Washington University in St. Louis  
Saint Louis, Missouri 63130 (USA)  
Fax: (+1) 314-935-7448  
E-mail: xia@biomed.wustl.edu

[b] Dr. H.-Y. Tuan  
Department of Chemical Engineering  
National Tsing Hua University, Hsinchu 300  
Taiwan (Republic of China)

[c] Prof. B. A. Korgel  
Department of Chemical Engineering  
University of Texas at Austin  
Austin, Texas 78712 (USA)

widely used hydrides, have proven to be effective for synthesizing Au nanoparticles. Additionally, various capping ligands, including alkanethiols,<sup>[15,21]</sup> alkylamines,<sup>[17,22]</sup> and polymers,<sup>[23]</sup> together with different preparation techniques, such as wet chemical synthesis,<sup>[15]</sup> radiolysis,<sup>[24]</sup> sonochemical approach,<sup>[25]</sup> and the UV irradiation method,<sup>[26]</sup> have all been extended to the synthesis of Au nanoparticles.

Although both Au<sup>III</sup> and Au<sup>I</sup> are common oxidation states of gold, precursors for the synthesis of Au nanoparticles are mainly based on Au<sup>III</sup> derivatives, in particular, HAuCl<sub>4</sub>. To date, Au<sup>I</sup> compounds have rarely been explored as precursors for generating Au nanoparticles. However, it has been proposed that Au<sup>I</sup> as an intermediate state may play a critical role in controlling the morphology of Au nanostructures synthesized from Au<sup>III</sup> ions.<sup>[27]</sup> In addition, Liz-Marzán and co-workers have showed that Au<sup>III</sup> may oxidize Au<sup>0</sup> in the presence of cetyltrimethylammonium bromide (CTAB) to alter the morphology of the Au nanoparticles.<sup>[28]</sup> Therefore, understanding the reduction of Au<sup>I</sup> into elemental Au would be helpful to achieve a better control of the size, shape, and crystallinity for the Au nanoparticles. It has been demonstrated that reduction of a Au<sup>I</sup> alkylphosphine complex, [AuCl(PR<sub>3</sub>)], by B<sub>2</sub>H<sub>6</sub> could lead to the formation of Au<sub>55</sub> clusters.<sup>[29]</sup> In an attempt to make Au nanoparticles from Au<sup>I</sup> species, Nakamoto and co-workers showed that thermolysis of Au<sup>I</sup> complexes, such as [C<sub>14</sub>H<sub>29</sub>N(CH<sub>3</sub>)<sub>3</sub>][Au(SC<sub>12</sub>H<sub>25</sub>)<sub>2</sub>] or [Au(C<sub>13</sub>H<sub>27</sub>COO)(PPh<sub>3</sub>)] at 180 °C could yield Au nanoparticles with sizes around 26 nm.<sup>[30]</sup> Chaudret and co-workers also found that Au<sup>I</sup> alkylamine complexes, derived from [AuCl(tetrahydrothiophene)] complex from its reaction with primary amines, could self-assemble on a substrate and form Au nanoparticles.<sup>[31]</sup> For both cases, however, control over the nanoparticle growth could hardly be achieved as the reaction conditions require either a high temperature or decomposition on a substrate. The special procedures required for preparing these complexes also limit their wide use as Au precursors. Most recently, Stucky and co-workers demonstrated that Au nanoparticles with relatively narrow polydispersity could be obtained from [AuCl(PPh<sub>3</sub>)] complex by using *tert*-butylamine borane as a reductant.<sup>[32]</sup>

Au<sup>I</sup> halides, such as AuCl and AuBr, are readily available and their rich chemistry has long been recognized.<sup>[33]</sup> Even though the low solubility in most solvents limited their use in the synthesis of Au nanoparticles, AuCl and AuBr can form soluble complexes with many ligands, such as alkenes,<sup>[34]</sup> alkylamines,<sup>[35]</sup> and alkylphosphines,<sup>[36]</sup> and these complexes in turn can serve as Au precursors. Both AuCl and AuBr exhibit relatively low stability under ambient conditions and can undergo disproportionation to form Au<sup>0</sup> and Au<sup>III</sup> species even at room temperature. The low stability of AuCl, AuBr, and their derivatives makes it possible to prepare Au nanoparticles under desirable mild reaction conditions without a reducing agent. The low reaction temperatures, the improved solubility of their complexes in various solvents, and the independence of any reducing agent would provide great flexibility for the preparation of Au nanostructures

from Au<sup>I</sup> halides for various applications. Herein, we report our investigation on the use of AuCl and AuBr as Au precursors to synthesize Au nanoparticles with alkylamine (either oleylamine or octadecylamine) as the coordinating agent and stabilizer. It is found that Au<sup>I</sup> halides can be dissolved in many organic solvents including chloroform by forming a complex with oleylamine or octadecylamine. When heated to a relatively low temperature of 60 °C, the Au<sup>I</sup>-alkylamine complexes gave rise to Au nanoparticles with a narrow size distribution.

## Results and Discussion

**Au nanoparticles made from AuCl and oleylamine:** Figure 1 shows TEM images of the Au nanoparticles synthesized from AuCl and oleylamine at 60 °C, with chloroform as the solvent. After washing with acetone, the nanoparticles were precipitated out by centrifugation and they are readily dispersible in solvents, such as chloroform and hexane. The Au nanoparticles synthesized by this procedure exhibited a relatively narrow size distribution without size-selective separation. The average diameter of the nanoparticles was 12.7 nm with a standard deviation of 8% relative to the mean diameter for the sample obtained from the chloroform solution with 20 mM AuCl and 0.4 M oleylamine. The high-resolution

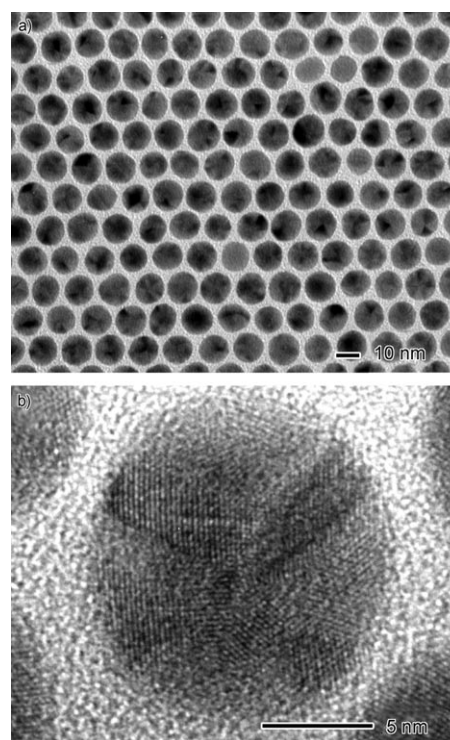


Figure 1. a) TEM image of Au nanoparticles synthesized at 60 °C from AuCl and oleylamine in CHCl<sub>3</sub>. The concentration of AuCl and oleylamine, respectively, was 20 mM and 0.4 M. The average diameter of the particles was 12.7 nm with a relative narrow size distribution of 8%. b) HRTEM revealing the multiple-twinning structure for the Au nanoparticles.

TEM images of the nanoparticles revealed a multiply twinned structure, typical for nanoparticles of Au and other noble metals with a face-centered cubic structure at small sizes. The yield of the nanoparticles was  $\approx 80\%$  when the reaction was stopped at 24 h, indicating that the majority of the AuCl had been converted to Au<sup>0</sup> and further incorporated into Au nanoparticles.

Figure 2 compares the FTIR spectra for oleylamine, the complex formed from oleylamine and AuCl, and the Au nanoparticles. The spectrum of oleylamine is characterized

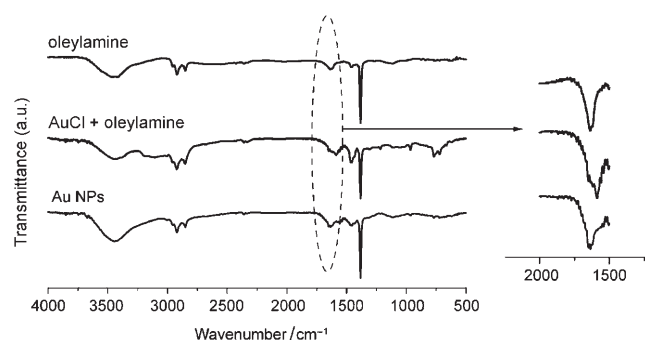


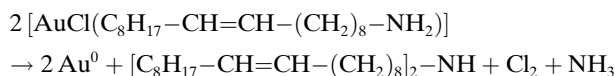
Figure 2. FTIR spectra of oleylamine, [AuCl(oleylamine)] complex, and Au nanoparticles capped with oleylamine. Note that the C=C stretch mode shifted from  $\tilde{\nu}=1640\text{ cm}^{-1}$  for oleylamine to a lower frequency of  $\tilde{\nu}=1590\text{ cm}^{-1}$  for AuCl and oleylamine complex is due to the coordination of C=C with AuCl. The C=C stretch mode for oleylamine-capped Au nanoparticles obtained by decomposing AuCl and oleylamine complex, however, was at the same frequency ( $\tilde{\nu}=1640\text{ cm}^{-1}$ ) as free oleylamine.

by bands at  $\tilde{\nu}=3450\text{ cm}^{-1}$  for the N–H stretch mode,  $\tilde{\nu}=1640\text{ cm}^{-1}$  for the C=C stretch mode, and  $\tilde{\nu}=1380\text{ cm}^{-1}$  for the CH<sub>2</sub> bending mode, in addition to the typical C–H stretch near  $\tilde{\nu}=2850\text{--}2960\text{ cm}^{-1}$ . When the oleylamine was mixed with AuCl in chloroform and a [AuCl(oleylamine)] complex had formed, the spectrum was nearly identical to that of the oleylamine, except that the C=C stretch mode was shifted to  $\tilde{\nu}=1590\text{ cm}^{-1}$  from the original  $\tilde{\nu}=1640\text{ cm}^{-1}$  for oleylamine. This shift could be attributed to coordination between the C=C bond of oleylamine and AuCl. Generally, the complexes formed from AuCl and alkenes are not stable and they may rapidly decompose at room temperature. The decomposition of [AuCl(oleylamine)] complex at 60 °C, however, did not complete in 24 h. This additional stability might be provided by the amine group through the formation of a N–H⋯Cl hydrogen bond.<sup>[35]</sup> Upon heating, the [AuCl(oleylamine)] complex decomposed to generate Au nanoparticles. The C=C stretch for Au nanoparticles shifted back to  $1640\text{ cm}^{-1}$ , at the same wavenumber as the C=C in oleylamine, indicating the disassociation of the C=C bond from the complex.

The formation of [AuCl(oleylamine)] complex was also confirmed by using MS analysis. The MS in the positive-ion mode for the mixture of AuCl and oleylamine in chloroform

exhibited three peaks at  $m/z$ : 268.3 for oleylamine, 464.3 for [Au<sup>I</sup>(oleylamine)]<sup>+</sup>, and 500.3 for [AuCl(oleylamine)] before the reaction (Figure 3a). The combined peak intensity for [Au<sup>I</sup>(oleylamine)]<sup>+</sup> and [AuCl(oleylamine)] is one fourth of the peak intensity for oleylamine, which is consistent with the starting molar ratio of oleylamine to AuCl at 5:1 for this sample. Once the reaction started at 60 °C, the intensity of [Au<sup>I</sup>(oleylamine)]<sup>+</sup> and [AuCl(oleylamine)] decreased and another peak at  $m/z$ : 516.5 started to appear. After 8 h, the relative peak intensity for  $m/z$ : 464.3 decreased to about half of its original value, and the intensity for the peak at  $m/z$ : 516.5 became stronger than the peak at  $m/z$ : 464.3 for oleylamine and AuCl complex (Figure 3b). With the increase of reaction time, the intensity of the  $m/z$ : 464.3 peak continued to decrease, while the peak intensity at  $m/z$ : 516.5 continued to increase. When the reaction was stopped at 24 h, the peak at  $m/z$ : 464.3 nearly disappeared (Figure 3c).

The fragmentation spectrum for the peak at  $m/z$ : 516.5 was obtained in the positive mode (Figure 3d). The resultant spectrum shows two major peaks at  $m/z$ : 266.3 and 280.4, which can be attributed to [C<sub>8</sub>H<sub>17</sub>–CH=CH–(CH<sub>2</sub>)<sub>8</sub>–NH]<sup>+</sup> and [C<sub>8</sub>H<sub>17</sub>–CH=CH–(CH<sub>2</sub>)<sub>8</sub>–NH–CH<sub>2</sub>]<sup>+</sup>, respectively. Therefore, the peak at  $m/z$ : 516.5 can be assigned to molecular dioleylamine [C<sub>8</sub>H<sub>17</sub>–CH=CH–(CH<sub>2</sub>)<sub>8</sub>]<sub>2</sub>–NH. Based on the experimental observation and spectroscopic analysis, we propose the following reaction mechanism for the formation of Au nanoparticles:



When the [AuCl(oleylamine)] complex was heated up to 60 °C in chloroform, a slow thermolysis occurred. The [AuCl(oleylamine)] complex decomposed to give elemental Au<sup>0</sup> and the oleylamine in the complex condensates to form dioleylamine. The Au<sup>0</sup> atoms nucleated and grew into nanoparticles stabilized by oleylamine and/or dioleylamine. The mechanism for the formation of dioleylamine remains unclear but it may be attributed to the strong noncovalent Au<sup>I</sup>–Au<sup>I</sup> interaction between two [AuCl(oleylamine)] complexes due to the hybridization and relativistic effect.<sup>[37,38]</sup> This so-called “aurophilic” interaction has been recognized as being responsible for the aggregation of Au<sup>I</sup>–thiolate complexes,<sup>[39]</sup> and it has also been observed in Au<sup>I</sup>–amine complexes.<sup>[35,38]</sup>

The reaction was closely monitored as the [AuCl(oleylamine)] complex decomposed and the formation of Au nanoparticles proceeded. Figure 4 shows the TEM images of the Au nanoparticles obtained at different reaction times. When the reaction was stopped at 3 h, very few Au nanoparticles were found. The size of the nanoparticles was  $\approx 4.1\text{ nm}$ , much smaller than those obtained after 24 h. With the progress of the reaction, the size of the Au nanoparticles increased. At 6, 12, and 18 h, the average diameter of the Au nanoparticles became 5.8, 9.2, and 10.1 nm, respectively. The diameter reached 12.7 nm when the reaction was stop-

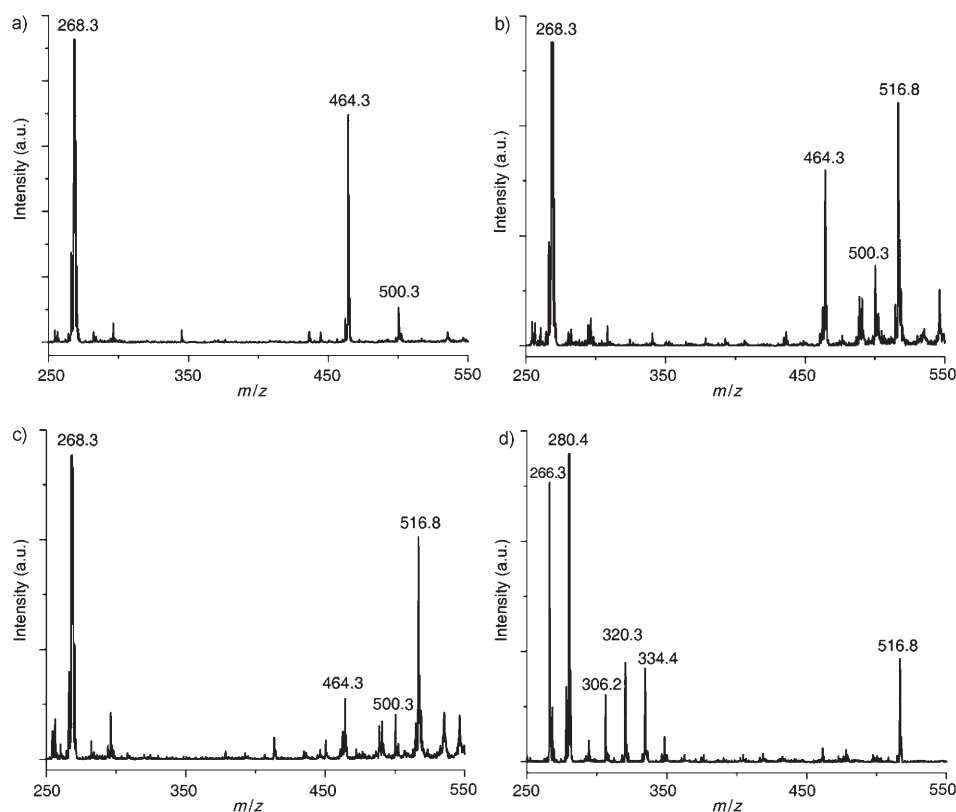


Figure 3. Mass spectra for  $[\text{AuCl}(\text{oleylamine})]$  complex before and after heating up to  $60^\circ\text{C}$  in  $\text{CHCl}_3$ , a) Once mixed, the  $\text{AuCl}$  and oleylamine formed a complex of  $[\text{AuCl}(\text{oleylamine})]$ , as confirmed by the peaks at  $m/z$ : 464 for  $[\text{Au}^{\text{I}}(\text{oleylamine})]^+$  and  $m/z$ : 500 for  $[\text{AuCl}(\text{oleylamine})]$ , respectively. b) After heating to  $60^\circ\text{C}$  in  $\text{CHCl}_3$  for 8 h, the peak intensity for the  $[\text{AuCl}(\text{oleylamine})]$  complex decreased, while another peak at  $m/z$ : 516.5 appeared. c) With the progress of the reaction, the peak intensity of  $[\text{AuCl}(\text{oleylamine})]$  complex continued to decrease and the peak intensity of  $m/z$ : 516.5 continued to increase. At 24 h, the peak at  $m/z$ : 464.3 was barely observable, indicating that most of the  $[\text{AuCl}(\text{oleylamine})]$  complex had decomposed. d) The MS/MS fragmentation for the peak at  $m/z$ : 516.5. Note that the molar ratio of oleylamine to  $\text{AuCl}$  for MS samples was 5:1. The intensities for oleylamine in (a), (b), and (c) were cut to adapt to the intensity of the complex.

ped at 24 h. When the reaction time was further prolonged, the size distribution decreased because of the involvement of Oswald ripening.

During the reaction process, the color of the solution changed gradually from clear to pink, indicating the slow decomposition of  $[\text{AuCl}(\text{oleylamine})]$  and formation of Au nanoparticles. The UV/Vis spectra of the Au nanoparticles obtained at different reaction times are presented in Figure 5. As mentioned above,  $\text{Au}^{\text{I}}$  halide compounds are generally unstable and they tend to disproportionate to form  $\text{Au}^0$  and  $\text{Au}^{\text{III}}$ . However, disproportionation of  $[\text{AuCl}(\text{oleylamine})]$  complex was not observed when it was heated up to  $60^\circ\text{C}$  in chloroform, as no absorption band for an  $\text{Au}^{\text{III}}$  species, typically at  $\lambda = 330$  nm, was observed during the progress of the reaction. The absorption maximum at  $\lambda = 530$  nm, a peculiar characteristic of the localized surface plasmon resonance peak of Au colloids, started to appear after three hours of reaction and the intensity increased steadily with the progress of the reaction, consistent with the observation by TEM, showing both the size and the number of particles increased with the reaction time.

To optimize the synthesis, reactions with various concentrations of  $\text{AuCl}$  and molar ratios of oleylamine to  $\text{AuCl}$  were investigated. Figure 6 shows the TEM images of the Au nanoparticles formed by varying the reaction conditions. It was found that a narrow size distribution ( $<10\%$ ) could only be achieved for the nanoparticles when the molar ratio of oleylamine to  $\text{AuCl}$  was above 20. Further increases of the molar ratio of oleylamine to  $\text{AuCl}$  to 30 did not change the size distribution. When the molar ratio is below 20, the nanoparticles exhibited polydispersity. For example, the sizes of the nanoparticles formed at an oleylamine/ $\text{AuCl}$  molar ratio of 5 and 10 showed the relative standard deviation of 28 and 18%, respectively, much higher than 8% for the nanoparticles obtained at an oleylamine to  $\text{AuCl}$  molar ratio of 20. Once formed, the Au nanoparticles are well protected by the oleylamine and they can be readily dispersed in many organic solvents including chloroform, hexane, and toluene, even after multiple washings.

**Octadecylamine as the stabilizer:** During the formation of Au nanoparticles from  $\text{AuCl}$ , oleylamine serves as both the complexing agent and capping ligand. In addition to oleylamine, octadecylamine was also employed as the stabilizer to grow Au nanoparticles. Figure 7a shows a TEM image of Au nanoparticles formed from the reaction of 20 mM  $\text{AuCl}$  in chloroform with a molar ratio of octadecylamine to  $\text{AuCl}$  of 20. Although octadecylamine and oleylamine exhibit similar basicity and affinity to metals caused by the  $\text{NH}_2$  group, the morphologies of the Au nanoparticles obtained from them are significantly different. The particles formed with octadecylamine showed an average size of  $\approx 100$  nm, 8 times larger than that of the particles made from oleylamine. A similar observation has been reported by Zurcher and co-workers in the synthesis of Co nanorods.<sup>[40]</sup> In their study, when oleylamine and octadecylamine were used as the capping ligands, the resultant Co nanorods showed different sizes, aspect ratios, and polydispersities. The difference was attributed to the supramolecular organization and/or dynamics of the ligands in solution, as oleylamine exhibits a "cis" configuration, leading to a shorter extended distance in solution.

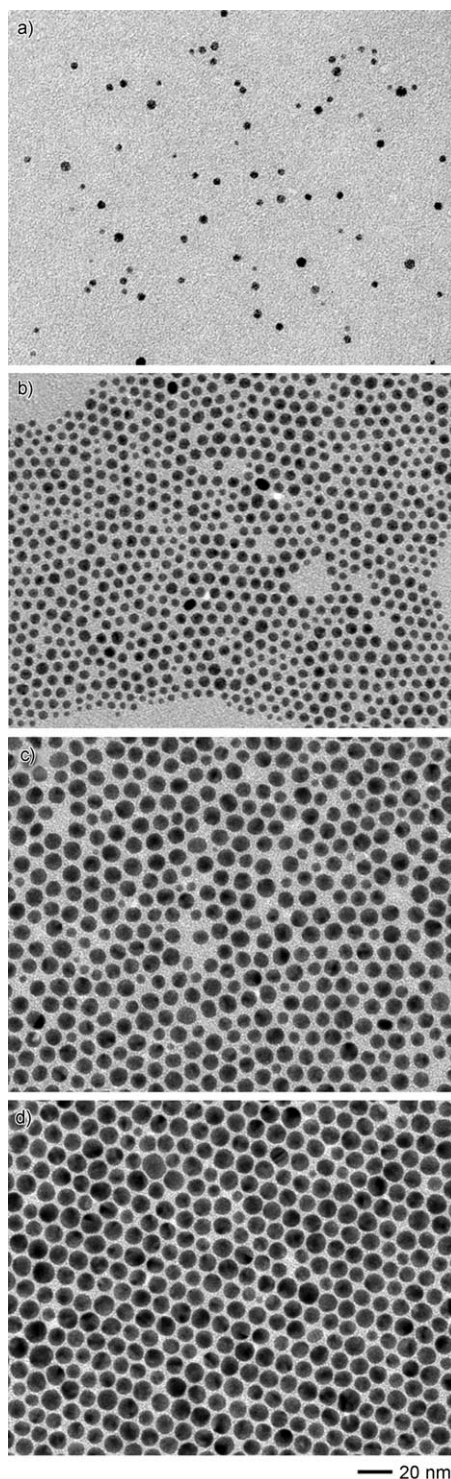


Figure 4. Morphological evolution of the Au nanoparticles obtained from 20 mM AuCl with 0.4 M oleylamine at different reaction times: a)  $t=3$  h,  $d=4.1$  nm; b)  $t=6$  h,  $d=5.8$  nm; c)  $t=12$  h,  $d=9.2$  nm; and d)  $t=18$  h,  $d=10.1$  nm. The size distribution decreased with the reaction time.

In the present case, however, a different mechanism is expected because if the molecular length is the determining factor for the morphology of the nanoparticles, the product obtained from oleylamine should be larger than those made

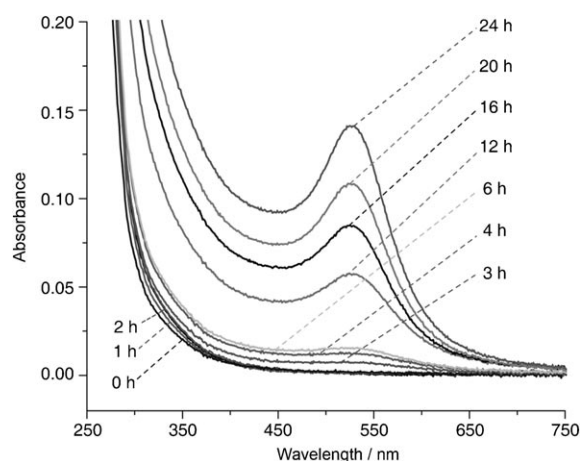


Figure 5. UV/Vis absorption spectra for the decomposition of AuCl in  $\text{CHCl}_3$  with the presence of oleylamine showing the intensity of the surface plasmon resonance peak gradually increases with reaction time.

from octadecylamine. As revealed by the FTIR spectra, the oleylamine can form a complex with AuCl through the C=C bond. The lack of C=C in octadecylamine will limit its coordination with AuCl to the amine group. Even though both C=C and amine groups can form complexes with AuCl,<sup>[34,35]</sup> study of the coordination between Au<sup>+</sup> and C<sub>2</sub>H<sub>4</sub> and NH<sub>3</sub> has shown that the bond strength of [Au(CH<sub>2</sub>=CH<sub>2</sub>)]<sup>+</sup> is larger than that of [Au(NH<sub>3</sub>)]<sup>+</sup>.<sup>[39,41]</sup> Accordingly, the complex formed from AuCl and oleylamine would be more stable than the complex formed from AuCl and octadecylamine. Additional stabilization can also be provided by the secondary interactions from the amine group.<sup>[35]</sup> The higher stability of [AuCl(oleylamine)] complex will cause slower decomposition and thus a slower growth rate for the Au nanoparticles when oleylamine instead of octadecylamine is used in the reaction. In addition, according to the study by Sastry and co-workers for the interactions between amine molecules and Au nanoparticles,<sup>[42]</sup> there exist two different modes of bonding: i) weak electrostatic interactions involving the protonated amine molecules and the chloraurate ions on the surface of the nanoparticles and ii) strong complexation in the form of Au<sup>0</sup>[AuCl(NH<sub>2</sub>R)]<sub>m</sub>. In the case of AuCl, as chloraurate ions could not be formed, the stabilization of Au nanoparticles is mainly due to the formation of [AuCl(NH<sub>2</sub>R)] complex. Therefore, more stable [AuCl(oleylamine)] complex may provide better passivation to the Au nanoparticles, and, therefore, smaller sizes and a narrower size distribution than the samples from the [AuCl(octadecylamine)] complex.

**AuBr as the Au precursor:** In addition to AuCl, another Au<sup>I</sup> halide, AuBr was also tested as the precursor to form Au nanoparticles. Similar to AuCl, AuBr is able to form a complex with oleylamine when chloroform is used as the solvent. When heated up to 60 °C in chloroform, the [AuBr(oleylamine)] complex decomposed gradually and the color of the solution turned from colorless to dark red. The reaction rate for AuBr to form Au nanoparticles is much higher than

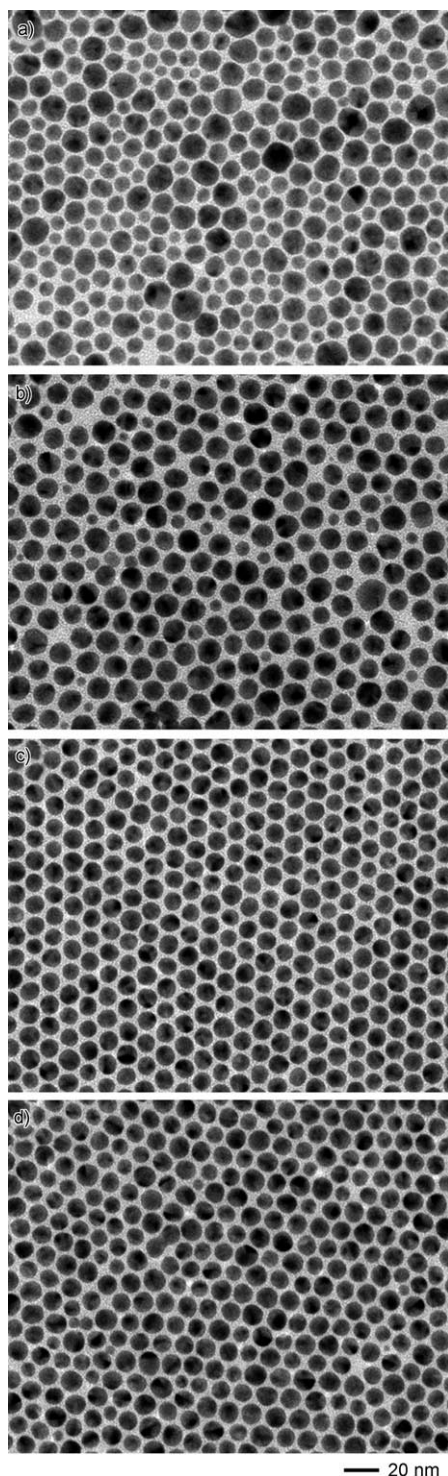


Figure 6. TEM images of Au nanoparticles obtained from the reaction of AuCl with different concentrations in  $\text{CHCl}_3$  at  $60^\circ\text{C}$  with oleylamine as the capping ligand. a)  $[\text{AuCl}] = 20 \text{ mM}$ , oleylamine/AuCl 5:1; b)  $[\text{AuCl}] = 20 \text{ mM}$ , oleylamine/AuCl 10:1; c)  $[\text{AuCl}] = 10 \text{ mM}$ , oleylamine/AuCl 20:1; and d)  $[\text{AuCl}] = 50 \text{ mM}$ , oleylamine/AuCl 20:1. A narrow size distribution could only be achieved when the molar ratio of oleylamine to AuCl was above 20.

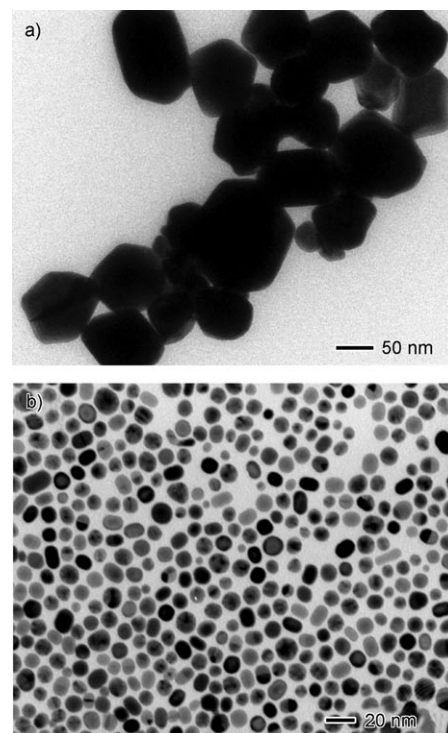


Figure 7. TEM images of Au nanoparticles obtained from the reaction of a) AuCl with octadecylamine and b) AuBr with oleylamine in  $\text{CHCl}_3$  at  $60^\circ\text{C}$ . While Au nanoparticles made from  $20 \text{ mM}$  AuCl and  $0.4 \text{ M}$  oleylamine were  $\approx 12 \text{ nm}$  in size, the particles made from  $20 \text{ mM}$  AuCl and  $0.4 \text{ M}$  octadecylamine in  $\text{CHCl}_3$  at the same reaction temperature had an average size of  $\approx 100 \text{ nm}$ . This result indicates that the C=C bond of oleylamine plays a critical role in stabilizing the nanoparticles and controlling their size. The decomposition of  $[\text{AuBr}(\text{oleylamine})]$  complex was much faster than that of  $[\text{AuCl}(\text{oleylamine})]$ . It took only three hours to complete the reaction. The sample showed a mixture of spherical and rod-shaped particles with an average aspect ratio of  $\approx 1.28$ . For comparison, the aspect ratio for the Au nanoparticles made from AuCl was nearly 1.0.

that of AuCl; the reaction was completed in 3 h at  $60^\circ\text{C}$  instead of 24 h with AuCl as the precursor. Figure 7b shows the TEM image of the Au nanostructures formed from AuBr in the presence of oleylamine with chloroform as the solvent. Instead of forming only spherical nanoparticles as in the case of AuCl, the decomposition of AuBr produced a mixture of nanospheres and nanobars. The average aspect ratio for the particles is 1.28, while the aspect ratio for nanoparticles made from AuCl is nearly 1.0. The formation of nanobars can be attributed to the anisotropic growth induced by the Br. As noticed by Murphy and co-workers, the presence of bromide is critical to the formation of Au nanorods from the reduction of  $\text{HAuCl}_4$  with CTAB as the surfactant.<sup>[43]</sup> Our recent studies also showed that KBr can assist the growth of Au nanorods, Pt nanobars, and Pd nanorods and nanobars.<sup>[44]</sup> The one-dimensional growth of these nanostructures is probably related to the chemisorption of bromide on the seed to promote the formation of certain facets, such as {100} and {110}, followed by localized oxida-

tive etching on one specific face of the seed to initiate preferential growth on this face.

## Conclusion

We have successfully developed a facile wet chemical method for synthesizing Au nanoparticles with narrow size distribution by using Au<sup>I</sup> halide compounds. Both AuCl and AuBr have proven to be effective precursors for generating Au nanoparticles simply by thermolysis under mild reaction conditions without the need for any reducing agent. When coordinated with oleylamine, AuCl could decompose slowly at 60 °C in chloroform and controlled growth of Au nanoparticles was achieved. The average size of the Au nanoparticles was ≈12 nm in diameter with a low polydispersity of 8% when the molar ratio of oleylamine to AuCl was 20. The UV/Vis and mass spectrometry measurements during the reaction process revealed a slow thermolysis of the [AuCl(oleylamine)] complex to form Au nanoparticles and dioleylamine. When octadecylamine instead of oleylamine was used as the capping ligand, much larger particles with sizes around 100 nm were obtained. Although both capping ligands are similar in terms of the length of the hydrocarbon chains and the basicity, the oleylamine could form a more stable complex with AuCl than octadecylamine because the coordination bond between AuCl and C=C is believed to be stronger than that between AuCl and RNH<sub>2</sub>. The higher stability and thus slower decomposition of [AuCl(oleylamine)] than [AuCl(octadecylamine)] led to a better control over the size of Au nanoparticles in the presence of oleylamine. When AuBr was used as the Au precursor to decompose in chloroform in the presence of oleylamine, a mixture of nanospheres and nanobars with average aspect ratio of 1.28 was obtained, indicating that one-dimensional growth was promoted for the case of AuBr, possibly due to the effect of local oxidative etching caused by Br<sup>-</sup>. This one-step Au<sup>I</sup>-based preparation method is independent of reducing agent and is expected to find applications that require mild reaction conditions.

## Experimental Section

**Chemicals:** All solvents, including chloroform, hexane, and acetone were received from Fisher Scientific and used as-received. Gold(I) chloride (99.9%; obtained from Aldrich), and gold(I) bromide (obtained from City Chemicals) were stored in a desiccator to avoid moisture. Oleylamine (technical grade, 70%) and octadecylamine (99.0%) were obtained from Aldrich and used without further purification.

**Synthesis of Au nanoparticles from AuCl and AuBr:** In a typical reaction, AuCl (or AuBr) (0.01 g) was mixed in a glass vial (20 mL) with certain volumes of oleylamine and chloroform according to the desired concentrations. After agitating for two minutes, AuCl (or AuBr) was dissolved and a clear solution of Au<sup>I</sup> complex was formed. The solution of AuCl (or AuBr) was then heated up to 60 °C by using an oil bath with stirring. Upon completion of the reaction, the nanoparticles were precipitated out with acetone (5 mL), followed by centrifugation (3900 rpm, 5 min). The nanoparticles were then re-dispersed with chloroform (2 mL)

and washed with acetone (5 mL). The precipitated particles were dispersed in chloroform (2 mL). Synthesis of nanoparticles with octadecylamine followed the same procedures.

**Characterization:** The UV/Vis spectra were recorded with a Cary 50 UV/Vis spectrometer by using a quartz cuvette with an optical path length of 1 cm. The samples at different reaction times were prepared by diluting an aliquot of the reactant mixture (0.1 mL) with chloroform (3 mL). The FTIR spectra were collected by using a Bruker Vector 33 IR spectrometer by drop casting the sample solutions onto KBr pellets, followed by drying under vacuum. TEM studies were done with a Philips EM420T microscope operated at 120 kV by drop casting the particle dispersions on copper grids coated with formvar and carbon film (SPI, West Chester, PA). High-resolution TEM (HRTEM) images were obtained with a JEOL 2010F microscope operated at 200 kV accelerating voltage. Mass spectra were taken with a Bruker Esquire LC-ion trap mass spectrometer with electrospray ion source operating in a positive mode. For sample preparation, reactant mixture (5 μL) before or after the reaction was added into a vial and diluted with *iso*-propanol (5 mL).

## Acknowledgements

This work was supported in part by a Director's Pioneer Award from the NIH (1DPOD000798) and a research grant from the NSF (DMR-0451788). Y.X. is a Camille Dreyfus Teacher Scholar (2002–2007). X.L. is an INEST Postdoctoral Fellow supported by Philip Morris USA.

- [1] a) M. C. Daniel, D. Astruc, *Chem. Rev.* **2004**, *104*, 293–346; b) G. Schmid, B. Corain, *Eur. J. Inorg. Chem.* **2003**, 3081–3098.
- [2] a) P. Alivisatos, *Nat. Biotechnol.* **2004**, *22*, 47–52; b) J. L. West, N. J. Halas, *Curr. Opin. Biotechnol.* **2000**, *11*, 215–217.
- [3] a) T. Dadosh, Y. Gordin, R. Krahne, I. Khivrich, D. Mahalu, V. Frydman, J. Sperling, A. Yacoby, I. Bar-Joseph, *Nature* **2005**, *436*, 677–680; b) S. Pradhan, J. Sun, F. J. Deng, S. Chen, *Adv. Mater.* **2006**, *18*, 3279.
- [4] R. J. Tseng, J. X. Huang, J. Ouyang, R. B. Kaner, Y. Yang, *Nano Lett.* **2005**, *5*, 1077–1080.
- [5] T. Hasobe, H. Imahori, P. V. Kamat, T. K. Ahn, S. K. Kim, D. Kim, A. Fujimoto, T. Hirakawa, S. Fukuzumi, *J. Am. Chem. Soc.* **2005**, *127*, 1216–1228.
- [6] I. H. El-Sayed, X. H. Huang, M. A. El-Sayed, *Nano Lett.* **2005**, *5*, 829–834.
- [7] a) C. Sönnichsen, B. M. Reinhard, J. Liphardt, A. P. Alivisatos, *Nat. Biotechnol.* **2005**, *23*, 741–745; b) G. L. Liu, Y. Yin, S. Kunchakarra, B. Mukherjee, D. Gerion, S. D. Jett, D. G. Bear, J. W. Gray, A. P. Alivisatos, L. P. Lee, F. Q. F. Chen, *Nat. Nanotechnol.* **2006**, *1*, 47–52.
- [8] a) S. J. Park, T. A. Taton, C. A. Mirkin, *Science* **2002**, *295*, 1503–1506; b) J. J. Storhoff, A. D. Lucas, V. Garimella, Y. P. Bao, U. R. Muller, *Nat. Biotechnol.* **2004**, *22*, 883–887.
- [9] a) M. Haruta, M. Date, *Appl. Catal. A* **2001**, *222*, 427–437; b) D. Astruc, F. Lu, J. R. Aranzacs, *Angew. Chem.* **2005**, *117*, 8062–8083; *Angew. Chem. Int. Ed.* **2005**, *44*, 7852–7872; c) M. Daté, M. Okumura, S. Tsubota, M. Haruta, *Angew. Chem.* **2004**, *116*, 2181–2184; *Angew. Chem. Int. Ed.* **2004**, *43*, 2129–2132; d) L. M. Molina, M. D. Rasmussen, B. Hammer, *J. Chem. Phys.* **2004**, *120*, 7673–7680.
- [10] M. Q. Zhu, L. Q. Wang, G. J. Exarhos, A. D. Q. Li, *J. Am. Chem. Soc.* **2004**, *126*, 2656–2657.
- [11] a) J. J. Storhoff, R. Elghanian, R. C. Mucic, C. A. Mirkin, R. L. Letsinger, *J. Am. Chem. Soc.* **1998**, *120*, 1959–1964; b) R. Elghanian, J. J. Storhoff, R. C. Mucic, R. L. Letsinger, C. A. Mirkin, *Science* **1997**, *277*, 1078–1081; c) J. Liu, Y. Lu, *Anal. Chem.* **2004**, *76*, 1627–1632.
- [12] a) O. Masala, R. Seshadri, *Annu. Rev. Mater. Res.* **2004**, *34*, 41–81; b) M. Brust, C. J. Kiely, *Colloids Surf.* **2002**, *202*, 175–186; c) Y. Yin, C. Erdonmez, S. Aloni, A. P. Alivisatos, *J. Am. Chem. Soc.* **2006**,

- 128, 12671–12673; d) Z. C. Xu, Y. L. Hou, S. H. Sun, *J. Am. Chem. Soc.* **2007**, *129*, 8698–8699.
- [13] M. Faraday, *Philos. Trans. R. Soc.* **1857**, *147*, 145–181.
- [14] J. Turkevich, P. C. Stevenson, J. Hillier, *Discuss. Faraday Soc.* **1951**, *11*, 55–75.
- [15] M. Brust, M. Walker, D. Bethell, D. J. Schiffrin, R. Whyman, *J. Chem. Soc. Chem. Commun.* **1994**, 801–802.
- [16] C. L. Chiang, *J. Colloid Interface Sci.* **2001**, *239*, 334–341.
- [17] a) D. V. Leff, L. Brandt, J. R. Heath, *Langmuir* **1996**, *12*, 4723–4730; b) H. Hiramoto, F. E. Osterloh, *Chem. Mater.* **2004**, *16*, 2509–2511; c) C. Subramaniam, R. T. Tom, T. Pradeep, *J. Nanopart. Res.* **2005**, *7*, 209–217; d) M. Aslam, L. Fu, M. Su, K. Vijayamohan, V. P. Dravid, *J. Mater. Chem.* **2004**, *14*, 1795–1797.
- [18] S. Ayyappan, R. S. Gopalan, G. N. Subbanna, C. N. R. Rao, *J. Mater. Res.* **1997**, *12*, 398–401.
- [19] C. E. Hoppe, M. Lazzari, I. Pardinias-Blanco, M. A. Lopez-Quintela, *Langmuir* **2006**, *22*, 7027–7034.
- [20] P. Mukherjee, A. Ahmad, D. Mandal, S. Senapati, S. R. Sainkar, M. I. Khan, R. Ramani, R. Parischa, P. V. Ajayakumar, M. Alam, M. Sastry, R. Kumar, *Angew. Chem.* **2001**, *113*, 3697–3700; *Angew. Chem. Int. Ed.* **2001**, *40*, 3585–3588.
- [21] a) M. Brust, J. Fink, D. Bethell, D. J. Schiffrin, C. Kiely, *J. Chem. Soc. Chem. Commun.* **1995**, 1655–1656; b) K. V. Sarathy, G. Raina, R. T. Yadav, G. U. Kulkarni, C. N. R. Rao, *J. Phys. Chem. B* **1997**, *101*, 9876–9880.
- [22] J. R. Heath, C. M. Knobler, D. V. Leff, *J. Phys. Chem. B* **1997**, *101*, 189–197.
- [23] a) S. T. Selvan, J. P. Spatz, H. A. Klok, M. Moller, *Adv. Mater.* **1998**, *10*, 132–134; b) M. K. Corbierre, N. S. Cameron, M. Sutton, S. G. J. Mochrie, L. B. Lurio, A. Ruhm, R. B. Lennox, *J. Am. Chem. Soc.* **2001**, *123*, 10411–10412.
- [24] a) E. Gachard, H. Remita, J. Khatouri, B. Keita, L. Nadjio, J. Belloini, *New J. Chem.* **1998**, *22*, 1257–1265; b) A. Henglein, D. Meisel, *Langmuir* **1998**, *14*, 7392–7396.
- [25] a) Y. Nagata, Y. Mizukoshi, K. Okitsu, Y. Maeda, *Radiat. Res.* **1996**, *146*, 333–338; b) W. Chen, W. P. Cai, L. Zhang, G. Z. Wang, L. D. Zhang, *J. Colloid Interface Sci.* **2001**, *238*, 291–295.
- [26] Y. Zhou, C. Y. Wang, Y. R. Zhu, Z. Y. Chen, *Chem. Mater.* **1999**, *11*, 2310.
- [27] a) C. C. Li, K. L. Shuford, Q. H. Park, W. P. Cai, Y. Li, E. J. Lee, S. O. Cho, *Angew. Chem.* **2007**, *119*, 3328–3332; *Angew. Chem. Int. Ed.* **2007**, *46*, 3264–3268; b) A. Halder, N. Ravishankar, *J. Phys. Chem. B* **2006**, *110*, 6595–6600.
- [28] J. Rodriguez-Fernandez, J. Perez-Juste, P. Mulvaney, L. M. Liz-Marzan, *J. Phys. Chem. B* **2005**, *109*, 14257–14261.
- [29] G. Schmid, *Chem. Rev.* **1992**, *92*, 1709–1727.
- [30] M. Nakamoto, M. Yamamoto, M. Fukusumi, *Chem. Commun.* **2002**, 1622–1623.
- [31] S. Gomez, K. Philippot, V. Colliere, B. Chaudret, F. Senocq, P. Le-cante, *Chem. Commun.* **2000**, 1945–1946.
- [32] N. Zheng, J. Fan, G. D. Stucky, *J. Am. Chem. Soc.* **2006**, *128*, 6550–6551.
- [33] *Chemistry of gold* (Ed.: R. J. Puddephatt), Vol. 16, Elsevier, New York, **1982**.
- [34] R. Hüttel, H. Reinheimer, H. Dietl, *Chem. Ber.* **1966**, *99*, 462–468.
- [35] P. G. Jones, B. Ahrens, *New J. Chem.* **1998**, *22*, 1041–1042.
- [36] A. Bayler, A. Schier, H. Schmidbaur, *Inorg. Chem.* **1998**, *37*, 4353–4359.
- [37] Y. Negishi, K. Nobusada, T. Tsukuda, *J. Am. Chem. Soc.* **2005**, *127*, 5261–5270.
- [38] B. Ahrens, P. G. Jones, A. K. Fischer, *Eur. J. Inorg. Chem.* **1999**, 1103–1110.
- [39] P. Pykkö, *Angew. Chem.* **2004**, *116*, 4512–4557; *Angew. Chem. Int. Ed.* **2004**, *43*, 4412–4456.
- [40] F. Dumestre, B. Chaudret, C. Amiens, M.-C. Fromen, M.-J. Casanove, P. Renaud, P. Zurcher, *Angew. Chem.* **2002**, *114*, 4462–4465; *Angew. Chem. Int. Ed.* **2002**, *41*, 4286–4289.
- [41] J. Hrusak, R. H. Hertwig, D. Schroder, P. Schwerdtfeger, W. Koch, H. Schwarz, *Organometallics* **1995**, *14*, 1284–1291.
- [42] A. Kumar, S. Mandal, P. R. Selvakannan, R. Pasricha, A. B. Mandale, M. Sastry, *Langmuir* **2003**, *19*, 6277–6282.
- [43] C. J. Murphy, T. K. San, A. M. Gole, C. J. Orendorff, J. Gao, L. Gou, S. E. Hunyadi, T. Li, *J. Phys. Chem. B* **2005**, *109*, 13857–13870; J. Gao, C. M. Bender, C. J. Murphy, *Langmuir* **2003**, *19*, 9065–9070.
- [44] Y. Xiong, H. Cai, B. J. Wiley, J. Wang, M. J. Kim, Y. Xia, *J. Am. Chem. Soc.* **2007**, *129*, 3665–3675.

Received: October 6, 2007

Published online: December 4, 2007